Abbreviations list

ECG, electrocardiogram; EEG, electroencephalogram; ORX-KO, prepro-orexin knockout; WT, wild type

Abstract

Our series of rat experiments have shown that locomotor activity, arousal level, body and brown adipose tissue temperatures, heart rate and arterial pressure increase episodically in an integrated manner approximately every 100 min (ultradian manner). Although it has been proposed that the integrated ultradian pattern is a fundamental biological rhythm across species, there are no reports of the integrated ultradian pattern in species other than rats. The aim of the present study was to establish a mice model using simultaneous recording of locomotor activity, eating behaviour, body temperature, heart rate and arousal in order to determine whether their behaviour and physiology are organised in an ultradian manner in normal (wild type) mice. We also incorporated the same recording in prepro-orexin knockout mice to reveal the role of orexin in the brain mechanisms underlying ultradian patterning. The orexin system is one of the key conductors required for coordinating autonomic functions and behaviours, and thus may contribute to ultradian patterning. In wild type mice, locomotor activity, arousal level, body temperature and heart rate increased episodically every 93±18 min (n=8) during 24 hours. Eating was integrated into the ultradian pattern, commencing 23±4 min (n=8) after the onset of an EEG ultradian episode. The integrated ultradian pattern in wild type mice is very similar to that observed in rats. In prepro-orexin knockout mice, the ultradian episodic changes in locomotor activity, EEG arousal indices and body temperature were significantly attenuated, but the ultradian patterning was preserved. Our findings support the view that the ultradian pattern is common across species. The present results also suggest that orexin contributes to driving ultradian episodic changes, however, this neuropeptide is not essential for the generation of the ultradian pattern.

Keywords

ultradian, orexin knockout mice, body temperature, arousal level, hypothalamus

Introduction

Circadian variation in behavioural and physiological parameters is well established. What is not so well recognized is the integrated fashion in which each parameter varies within each phase of the day/night cycle as the animal alternates between inactive and active states (Richter, 1927, Honma and Hiroshige, 1978, Shimada and Marsh, 1979, Livnat et al., 1984, Stupfel et al., 1985, Alfoldi et al., 1990, Holstein-Rathlou et al., 1995). It is proposed that, in addition to circadian patterning, ultradian (<24 hour) alternation between active interaction with the external environment and rest is a fundamental part of animal life (Aschoff and Gerkema, 1985, Ootsuka et al., 2011, Blessing et al., 2012, 2013, Blessing and Ootsuka, 2016). The ultradian pattern, also referred to as the basic-rest activity cycle (Kleitman, 1982), is particularly prominent when the circadian pattern is eliminated by destruction of the suprachiasmatic nucleus (Baker et al., 2005).

In rats, the integrated phase-linked behavioural and physiological changes, occurring every 1-2 hours (ultradian manner), commence with an increase in locomotor activity associated with an increase in hippocampal theta power, indicating alert attention to the external environment (Ootsuka et al., 2009, Buzsaki and Moser, 2013). Following this, within minutes, arterial pressure, heart rate, as well as body and brain temperature increase. Increases in temperature are partially due to increased brown adipose tissue (BAT) thermogenesis (Ootsuka et al., 2009, Blessing et al., 2012). Eating occurs during the active ultradian periods, commencing approximately 15 minutes after the onset of the theta rhythm-associated locomotor activity (Ootsuka et al., 2009, Blessing et al., 2012). Notably, the integrated ultradian pattern continues even under food-depravation (Blessing et al., 2012). These observations suggest that the ultradian pattern is centrally coordinated as opposed to a secondary phenomenon driven by external events, or by afferent signals originating peripherally.

Although the ultradian pattern is likely to be a fundamental biological rhythm across animal species (Aschoff and Gerkema, 1985, Ootsuka et al., 2011, Blessing et al., 2012, 2013), so far there are no reports of the integrated ultradian behavioural and physiological pattern in animals other than rats. Previous mice studies, which measured locomotor activity, body temperature, oxygen consumption, respiratory rhythm and arousal level not simultaneously but individually in the majority of cases, have shown

that these parameters increase in an ultradian episodic manner (Stupfel et al., 1985, Stupfel et al., 1990, Mazzucchelli et al., 1995, Stupfel et al., 1995, Poon et al., 1997, D'Olimpio and Renzi, 1998, Mochizuki et al., 2006, Dowse et al., 2010, Blum et al., 2014, Ono et al., 2015). To date, however, there are no reports of the integrated ultradian pattern in mice based on simultaneous recordings of multiple behavioural and physiological parameters. Thus, the first aim of this present study is to simultaneously record behavioural and physiological parameters in mice, in order to determine whether this species displays an integrated ultradian pattern similar to rats. This was done by assessing its intervals and temporal pattern as performed in our rat studies. The issue is particularly important because the wide variety of transgenic mice models provide invaluable opportunities for exploring the brain mechanisms responsible for generating and coordinating the ultradian pattern.

Our group has already studied the ultradian pattern in transgenic rats with ataxin-mediated destruction of the hypothalamic orexin/hypocretin neurons (Mohammed et al., 2014). Orexin has an important role in orchestrating multiple behavioural and physiological functions. (Chemelli et al., 1999, Nambu et al., 1999, Samson et al., 1999, Yamanaka et al., 1999, Chen et al., 2000, Antunes et al., 2001, Hara et al., 2001, Willie et al., 2001, Machado et al., 2002, Sakurai, 2007, Kuwaki, 2008, Tsujino and Sakurai, 2009, Inutsuka et al., 2014, Mahler et al., 2014, Sakurai, 2014, Bonnavion et al., 2015, Kuwaki, 2015). In mice this role has been investigated by experiments using prepro-orexin knockout (ORX-KO) animals that cannot produce orexin. In these mice, the amplitudes of behavioural and autonomic physiological responses to aversive events are reduced (Zhang et al., 2006b, Zhang et al., 2009, Zhang et al., 2010, Kuwaki, 2011). Wake-sleep patterns which show ultradian fluctuations in mice are dysregulated (Chemelli et al., 1999, Mochizuki et al., 2006). During the transition between wake-sleep states, physiological variables involving body temperature, heart rate and metabolic rate changed (Zhang et al., 2007, Bastianini et al., 2011, Lo Martire et al., 2012, Silvani et al., 2014). The changes are attenuated in ORX-KO mice (Mochizuki et al., 2006, Zhang et al., 2007). Arousal levels increase at the onset of active ultradian behavioural and autonomic episodes (Ootsuka et al., 2009). Thus, it is possible that orexin neurons integrate key circuits involved in coordinating the ultradian pattern. The ultradian pattern has been partly examined in ORX-KO mice (Mochizuki et al., 2006),

but there is otherwise little information concerning the role of orexin in generating and coordinating integrated ultradian behavioural and autonomic pattern.

Thus, the second aim of the present study is to simultaneously record behavioural and physiological parameters in ORX-KO mice, with attention to the occurrence of integrated ultradian behavioural and physiological patterns in these animals, in order to investigate the role of orexin in regulation of the ultradian pattern. In conscious, unrestrained animals, we made simultaneous recordings of locomotor activity, body temperature and heart rate using telemetric procedures. In a separate group, in addition to these parameters, we also recorded the EEG via a wired headpiece, as well as the timing and amount of food consumed. We employed continuous wavelet analysis (CWT) to assess the intervals between individual ultradian episodes.

Experimental Procedure

Ethics Approval

All experiments were conducted at Kagoshima University in accordance with the guiding principles for the care and use of animals in the field of physiological sciences published by the Physiological Society of Japan (revised in 2015) and with ethical approval from the Institutional Animal Use Committee at Kagoshima University. All efforts were made to minimize the number of animals used and their suffering.

Animals

Animals used in the study were male ORX-KO mice (30-53g, n=14) and WT littermates (30-50g, n=14). The ORX-KO mice (Chemelli et al., 1999) were provided by Professor Takeshi Sakurai (Kanazawa University, Japan), and bred at Kagoshima University. The genotype of ORX-KO was identified by polymerase chain reaction of DNA extracted from tail tissue samples (Terada et al., 2008, Zhang et al., 2009). Animals were operated on under general anaesthesia (2% isoflurane in air, Sumitomo Dainippon Pharma, Tokyo, Japan). After surgery, analgesia (Ketoprofen cream, Hisamitsu Pharmaceutical Co., Inc., Saga, Japan) was applied around incision areas, and an antibiotic (vancomycine hydrochloride, 30mg/kg s.c., Shionogi & Co., Ltd, Osaka, Japan) was administered. The animals were then maintained in quiet environments (a 12hr/12hr light-dark cycle, lights on at 0700h), and individually caged away from other mice with minimal human intrusions. Animals were allowed to recover for at least one week before experimental recordings were carried out. Standard food and water were available ad libitum.

Measurement of body temperature, heart rate, and cortical EEG

There were two experimental setups for both WT and ORX-KO mice. In one setup, the mice were unrestrained, with locomotor activity, body temperature, and heart rate measured telemetrically from a chronically implanted probe (telemetry-only). The other setup used a wired-recording system to measure EEG, in addition to the telemetry recording system (EEG-recording experimental group).

Body temperature and electro-cardiogram (ECG) for heart rate were measured using a telemetric transmitter (model ETA-F10, Data Sciences International (DSI), St.

Paul, MN, USA). The telemetered temperature and ECG signals were detected with a PhysioTel Receiver (RLA1020, DSI) and converted to analogue voltage signals with converters (Option R08 & R12, DSI).

In the second set of experiments, EEG was measured with a wired-recording system, in addition to telemetry recordings of body temperature, ECG and locomotor activity (see next section). For EEG recording, skull burr holes were made and stainless screws were fixed. Reference and ground electrodes were screwed into frontal and occipital bones, respectively. A signal electrode was screwed into the parietal bone at 1.5 mm lateral (left) and 2 mm posterior to Bregma. Copper wires were wrapped around the stainless screws and insulated with dental cement (Unifast Trad, GC Japan, Tokyo, Japan). Nylon-insulated copper wires from EEG screw electrodes were connected to a headpiece and fixed with dental cement. The EEG signal was filtered (0.53-48Hz) and amplified (x20) through a voltage-buffer amplifier (TL072CDT, STMicroelectronics Japan, Tokyo, Japan) attached to the head socket.

Measurement of locomotor activity and eating

In the telemetry-only experiment, infrared-light-beams (XY grid pattern, 4 cm apart) were used to measure animal locomotor activity. The infrared-light-beams generate a square analogue pulse (4V, 170 msec/detection) triggered by interruption of an infrared beam. In the EEG-recording experimental group, a pyro-electric passive infrared sensor (NaPiOn, AMN1111, Panasonic, Osaka, Japan) was used. The pyro-electric infrared sensor generates a square analogue pulse (3V, 30 msec/detection) when it detects changes in infrared radiation.

In the EEG-recording experimental group, the food container weight was measured. Five to six cylindrical food pellets (10 mm diameter and 30 mm long) were placed in a wire grid hemisphere container. The container grid size was approximately 7 mm x 27 mm. The mouse was able to access the food pellets by inserting its snout through the grid. The food container was suspended from a strain gauge (TB611T, Nihonkoden, Tokyo, Japan) and placed inside the experimental cage at approximately 4 cm from the bottom of the cage. Signals from the gauge were amplified with a bridge amplifier (AD-632J, Nihonkoden) and converted to weight units on data-capturing software. When the animal disturbed the container, a bout of large and abrupt intermittent changes were

evoked in strain gauge signals. Actual eating was defined as a decrease of > 0.05 g in the weight of the food container. The start and end of the meal were taken as the time of the first and the last disturbance of the food container, respectively. Food and water were available ad libitum during experimental recording.

Signal analysis of physiological records

All signals were digitized (100Hz for locomotor activity, 1kHz for EEG and ECG, 2Hz for body temperature, 1Hz for food container) with PowerLab (ADInstruments Inc., Bella Vista, NSW, Australia), and captured with Chart software (ADInstruments). Signal analysis was performed using IgorPro (Wavemetrics, Lake Oswego, OR, USA) and MATLAB (MathWorks, Natick, MA, USA). The locomotor activity signal was processed to uniform its pulse amplitude and then integrated (1 min time constant). Discrete-wavelet-based signal process was used to fit and smooth the original signals, as described previously (Ootsuka et al., 2009). Total amplitude of EEG frequency power between 1-20 Hz was calculated and expressed as 1 min average. Instantaneous heart rate was calculated from a R-R interval in the ECG and averaged over 10 sec intervals. When the R-R intervals could not be identified (due to noise in ECG), an appropriate value was interpolated with values at surrounding points.

Because ultradian episodic changes have large variation in both periodicity and amplitude, they are not effectively demonstrated by conventional stationarity-based analytical techniques, such as Fourier, cosinor periodogram and autocorrelation procedures (Blessing et al., 2013, Blessing and Ootsuka, 2016). Thus, we employed continuous wavelet analysis (CWT) to assess the intervals between individual ultradian episodes. CWT provides a localised frequency decomposition and therefore is useful for analysing non-stationary signals (Graps, 1995, Torrence and Compo, 1998) including ultradian variation in biological signals (Poon et al., 1997, Leise, 2013, Mohammed et al., 2014). We used CWT analysis to assess ultradian components in behavioural and physiological signals. We also employed the peak-method to assess peak-intervals and temporal pattern as performed in our rat studies (Ootsuka et al., 2009, Blessing et al., 2012) (Blessing and Ootsuka, 2016). For the peak-method of measurement, we first specified criteria for a peak and then measured the intervals between sequential ultradian peaks. To be defined as a peak, the increase in body temperature was required

to have an amplitude of at least 0.3 ºC, with an interpeak interval of at least 35 min, as previously defined (Ootsuka et al., 2009). Corresponding peaks in heart rate were identified within ±20 min of a given body temperature peak. Onset times of body temperature increases, corresponding heart rate increases and EEG Fourier-power decreases were defined using the body temperature peaks as reference (Ootsuka et al., 2009). We assessed the time relationship between onset values for each behavioural and autonomic parameter, as in our previous rat study (Blessing et al., 2012).

Experimental procedures

In the telemetry device-only experiment, a mouse in its home cage was transferred to a sound insulated and temperature-controlled room (24-26ºC), lights switched on at 0700 and off at 1900 at the beginning of the experimental period. In the EEG recording experiment, a mouse was transferred from his home cage to an experimental cage in the sound insulated and temperature-controlled room (24-26ºC). A flexible cable from a swivel device (SL6C+2, Plastics One Inc., Roanoke, VA, USA) was then attached to the mouse's head socket via the voltage-buffer amplifier. At least a 12-hour period was allowed for the animal to become habituated to the new environment. Continuous recording was then performed over 24 hours.

Statistical analysis

Statistical analysis was performed using SPSS (IBM Corp., Armonk, NY, USA). Group data were shown as mean ± SD for descriptive statistics and mean ± SEM for inferential statistics. Kolmogorov-Smirnov and Levene's tests was used to assess normal distributions and equal variance in sampled data. Mean values between WT and KO mice were compared using Student's unpaired t-test or Welch's t-test when equal variances were not assumed. Mann-Whitney's U test was used for unpaired samples that were not normally distributed. Paired t-test was used to analyze differences between the dark and light period values recorded in the same rat. Wilcoxon signed-rank test was used for paired samples that were not normally distributed. Linear regression analysis was performed in order to assess time-dependent changes in parameters before the commencement of disturbing a food container. The statistical significance of wavelet-power was assessed using software for wavelet analysis incorporating algorithms for

Brownian noise (red noise) in MATLAB (http://noc.ac.uk/using-science/crosswavelet-wavelet-coherence/) (Grinsted et al., 2004). The purpose of the statistical evaluation is to compare the actual spectrum against a random distribution (i.e. Brownian noise). When a peak in the wavelet power spectrum was above 95% confidence level calculated from the background noise, it was assumed to be a true phenomenon (Torrence and Compo, 1998).

Results

Ultradian patterning of body temperature, heart rate and locomotor activity in WT mice

Recordings from an individual mouse showing episodic increases in body temperature in association with increases in heart rate and locomotor activity, together with the CWT analysis of each parameter are presented in Fig. 1. Significant wavelet-power areas are indicated by the pink contours (see legend to Fig. 1). Significant ultradian episodic changes were observed throughout the 24-hour monitoring period in both light and dark cycles. Their periodicity ranged between 30 and 200 min.

We also employed the peak-method to evaluate inter-peak intervals and amplitudes of ultradian peaks as in our previous rat studies (Ootsuka et al., 2009, Blessing et al., 2012). Frequency distributions of the inter-peak intervals and amplitudes of body temperature (129 episodes during 24 hours in 8 mice) are shown in Fig. 2. The inter-peak intervals were widely distributed between 30 and 200 min, which were consistent with results from CWT analysis in which the Morlet wavelet detected both amplitude and frequency at given time points of the physiological signal (Price et al., 2008, Leise et al., 2013), and with the variability documented in our previous rats studies (Ootsuka et al., 2009, Blessing et al., 2012). For further analysis, inter-peak intervals, their amplitudes, and the basal value at the onset of each episode were averaged in each mouse, separately for light and dark periods. The averaged data sets from each mouse were then pooled across mice (Table 1). During the dark phase, the average inter-peak interval of episodic increases in body temperature was approximately 90 min. There were no significant differences in inter-peak intervals, amplitudes or basal values between light and dark phases (Table 1).

In the EEG-recording experimental group, CWT analysis showed similar significant ultradian changes in body temperature, heart rate and locomotor activity. The peak-method showed that episodic increases in body temperature during the dark phase occurred every 79±19 min (mean±SD, n=6), with amplitude 1.1±0.3 ºC (mean±SD, n=6). Student's unpaired t-test showed that the inter-peak intervals ($t(12)=0.968$, $P=0.352$) and the amplitudes ($t(12)=0.397$, $P=0.698$) were comparable to those observed in the telemetry-only group.

Body temperature and its temporal relationship with other physiological parameters in WT mice

Recordings from an individual mouse in the EEG-recording experimental group showed that every ultradian episodic increase in body temperature was associated with a decrease in EEG power (Fig 3), which is an index for increases in arousal level (Halasz et al., 2004). For each episodic increase in body temperature we selected 60 min segments commencing 30 min before the onset of the increase in body temperature, and ending 30 min after the onset. The body temperature segment and corresponding 60 min segments of the other physiological parameters with reference to the body temperature onset times were averaged for each mouse. The averaged data set from each mouse was pooled across mice. The results are shown with separate analyses for dark and light phases in Fig 4. Ultradian episodic increases in body temperature were preceded by a decrease in EEG power (6±1 min before the body temperature onset, mean±SD, n=6) and by an increase in heart rate (4±1 min before the onset, mean±SD, n=6) during the dark phase (Fig. 4). Locomotor activity began to increase at the onset of body temperature increases. These temporal relationships were similar in the dark and the light phases.

Eating and its temporal relationship with other physiological parameters in the WT mice

With food available ad libitum, all eating occurred in association with an ultradian episodic increase in body temperature (Figs 3 and 5A). Mice accessed food more frequently during the dark phase than during the light phase (Table 2). Similar amounts of food were consumed per meal during both phases (Table 2).

The timing of different physiological parameters averaged, with respect to the commencement of eating, are shown in Fig. 5A. Linear regression analysis showed a significant decrease in EEG Fourier-power ($F_{(1,28)}$=81.304, P<0.001), an increase in heart rate ($F_{(1,28)}$=34.257, P<0.001), body temperature ($F_{(1,28)}$=18.76, P<0.001) and locomotor activity ($F_{(1,28)}$=10.561, P=0.003), before the onset of eating during the dark phase. The significant changes in each parameter were also observed during the light phase ($F_{(1,28)}$=40.507, p<0.001 for EEG Fourier Power, $F_{(1,28)}$=56.431, p<0.001 for

heart rate, $F_{(1,28)}$=19.217, p<0.001 for body temperature, and $F_{(1,28)}$=14.425, p=0.001 for locomotor activity).

The onset times for physiological parameters were defined as occurring at the maximum value of the EEG Fourier-power during 30 min observation time prior to onset of eating, or as the minimum value of body temperature and heart rate during the 30 min. Before the onset of eating, EEG Fourier-power began to decrease at 22±3 min (mean±SD, n=6), and heart rate began to increase at 22±4 min (mean±SD, n=6). Body temperature began to increase at 17±5 min (mean±SD, n=6). These temporal patterns of the physiological and behavioural parameters were similar in dark and light phases.

Comparison of ultradian patterns in body temperature, heart rate, and locomotor activity between WT and ORX-KO mice

As shown in Fig. 1, WT mice displayed significant body temperature wavelet-power for the whole day, in both the light and dark phases. In contrast, as shown in Fig. 6, ORX-KO mice displayed significant body temperature wavelet-power for only a limited period of the day, transition from dark to light period (Fig. 6). We also calculated total wavelet-power amplitude from wavelet-power spectrum between 30 and 200 min periodicity ranges (Fig. 7). In the ORX-KO mice, the overall wavelet-power amplitude of the ultradian fluctuations during 24 hours was significantly reduced in body temperature (t(14)=3.746, P=0.002, Student's unpaired t-test), and in locomotor activity (t(14)=3.89, P=0.002, Student's unpaired t-test), compared with the WT mice. The ultradian wavelet-power amplitude for heart rate during 24 hours was similar both in the ORX-KO and the WT mice (P=0.645, Mann-Whitney U test).

ORX-KO mice showed frequent cataplexy episodes in the first half of the dark phase (Kaur et al., 2008). We divided each dark and light phase into two parts (i.e. the first 6 and the second 6 hours) for further comparison of the ultradian episodic fluctuations between the ORX-KO and WT mice (Fig. 7B). During the first half of the dark phase but not during the second half, the ultradian wavelet-power amplitude in heart rate of the ORX-KO mice was significantly less than that of WT mice (t(14)=3.267, P=0.006, Student's unpaired t-test).

Ultradian pattern in EEG power in the ORX-KO mice

Ultradian episodic decreases in EEG Fourier-power in the ORX-KO and the WT mice were evaluated by the CWT analysis (n=6). Both the ORX-KO mice (Fig 8) and the WT mice (Fig 3) showed a significant wavelet-power throughout a 24-hour observation time. The ultradian EEG wavelet-power amplitude was significantly less in ORX-KO mice than in WT mice during all four phases (Fig. 9).

Eating and its temporal relationship with other physiological parameters in the ORX-KO mice

Eating occurred episodically in the ORX-KO mice (Fig 8), as was the case in the WT mice. The ORX-KO (n=5) and the WT mice (n=6) accessed the food cage a similar number of times during the dark phase ($t(9)=1.204$, $P=0.259$, Student's unpaired t-test), but the ORX-KO accessed the food cage less frequently than the WT mice during the light phase ($P=0.030$, Mann-Whitney U test). The ORX-KO and WT mice consumed a similar amount of food per meal per body weight during each phase (Table 2).

For the ORX-KO mice, the timing of each physiological parameter averaged, with respect to the onset of eating during the dark phase, is shown in Fig. 5B. During the dark phase, EEG Fourier-power began to decrease at 16±7 min (mean±SD) before the onset of eating in 4 of 5 animals. In these 4 animals, heart rate began to increase at 15±10 min (mean±SD) before the onset of eating. These latencies did not differ from those in WT mice ($P=0.114$ for EEG latency, $P=0.352$ for heart rate latency, Mann-Whitney U test). In the 5 animals, Linear regression analysis showed no significant increases in body temperature ($F_{(1,23)}=0.578$, $P=0.455$) and in locomotor activity ($F_{(1,23)}=2.589$, $P=0.121$) before the onset of eating. These temporal patterns of the physiological variables and behavioural parameters were similar in both dark and light phases.

DISCUSSION

Phase-linked ultradian episodic changes in physiological parameters are present in wild type (WT) mice

The present study, utilising simultaneous recordings of different behavioural and physiological parameters, is the first to report integrated daily-life ultradian patterns in mice. The interval of the integrated behavioural and physiological changes was approximately 90 min. The changes commenced with a decrease in EEG Fourier power. The ultradian episodic changes were similar both in a telemetry recording and in a combined telemetry system with a wired recording, indicating that the wired-recording system did not adversely affect the mice. Importantly, the approximately 15 min latency to the commencement of eating after the initiation of the ultradian changes, previously documented in rats, was also present in mice. In rats, the phase-linked ultradian episodic changes, including accessing the food container, occur even under food-deprived conditions (Blessing et al., 2012), suggesting that food intake is a part of integrated ultradian episodic patterns. Ultradian episodic increases in body temperature also occur in mice and voles during food deprivation (Gerkema and van der Leest, 1991, Nieminen et al., 2013). Our findings are similar to those reported previously in rats (Ootsuka et al., 2009, Blessing et al., 2012). Thus, the present data is consistent with the view that the ultradian alternation of rest-active states is a fundamental part of animal life (Aschoff and Gerkema, 1985, Ootsuka et al., 2011, Blessing et al., 2012, 2013).

Previous studies, using EEG-based wake-sleep scoring, show robust changes in behavioural and physiological parameters upon waking (Mochizuki et al., 2006, Zhang et al., 2007, Bastianini et al., 2011, Lo Martire et al., 2012, Silvani et al., 2014, Bastianini et al., 2015). Zhang and colleagues performed simultaneous recording of different behavioural and physiological parameters in mice, including EEG and food intake, observed that eating occurs approximately 15 min after waking (Zhang et al., 2007). However, the investigators did not discuss ultradian patterning. A modified wake-sleep scoring has been used to show parallel ultradian patterns of wakefulness and body temperature in mice (Mochizuki et al., 2006). However, the investigators did not provide a detailed analysis of ultradian physiological changes. Wake states in mice last for only a few seconds or a few minutes (Bastianini et al., 2011). This implies that

analysis based on wake-sleep scoring can easily overlook ultradian patterning that occurs over a time period of hours.

Orexin neurons are important for driving the ultradian episode, while the neurons are not part of the ultradian oscillation network

Loss of orexin significantly attenuated the wavelet-power amplitude of ultradian episodic changes in body temperature, locomotor activity and EEG Fourier-power. Mochizuki and colleagues, using different methodology, also found attenuation of the ultradian fluctuation in ORX-KO mice (Mochizuki et al., 2006). In the present study, we also measured heart rate and eating in addition to those parameters and showed that the ultradian patterns of heart rate in ORX-KO mice were comparable to those in WT mice. Integration of eating into the ultradian pattern was still present in ORX-KO mice. The results indicate that the fundamental ultradian patterning is preserved in ORX-KO mice. Therefore, it is unlikely that the orexin system is part of the ultradian oscillation network. It is, instead, important for driving episodic changes and mediating their amplitude (see further discussion in the next section).

Ultradian modulation of the orexin level may contribute to stabilizing the ultradian episodic changes

Activity of orexinergic-like neurons is associated with wakefulness (Mileykovskiy et al., 2005). The amount of wakefulness changes in an ultradian manner in mice (Mochizuki et al., 2006). Thus, it is possible that orexin neuronal activity is modulated in an ultradian manner by receiving signals from the upstream ultradian oscillation network, thereby contributing to driving ultradian episodic changes. It has been proposed that the loss of orexin signal lowers thresholds between wake and sleep state alternations, and thereby may be lead to disintegration in the neurophysiological mechanism for stabilising transitions between the states (Mochizuki et al., 2004). Unstable states may impair stable ultradian-modulated outputs from orexin neurons to behavioural and physiological regulatory pathways. It remains to be investigated whether orexin neuronal activity and level of orexin peptide fluctuate in an ultradian manner.

The degree of vulnerability to the instability may be different between the pathways. Inputs to thermoregulatory pathways may be highly vulnerable to instability, resulting in almost no ultradian increases in body temperature, while those to cardiovascular regulatory pathways may be resistant. In ORX-KO mice, ultradian patterning in heart rate was disorganized only in the first half of the dark period. ORX-KO mice typically have cataplexic episodes in the first phase, suggesting a tendency to go into the unstable states during the first half phase than the others. More frequent random alternation between the states may become sufficient to cause disorganisation of ultradian signals that mediate heart rate during the first half dark phase.

Body temperature is maintained at a lower level during sleep in wild type mice (McGinty and Szymusiak, Mochizuki et al., 2006), while remaining at a high level during sleep in ORX-KO mice (Mochizuki et al., 2006). This suggests that the orexin system contributes to lowering body temperature as well as raising the temperature (Monda et al., 2001, Monda et al., 2004, Zheng et al., 2005). The orexin system may act as a selector switch to actively turn on or off heat dissipation or heat production mechanisms depending on dynamic ultradian modulation in orexin levels.

The present study demonstrates that orexin signals are more important for driving ultradian increases in temperature than heart rate. In contrast, the signals are important, not for thermoregulatory responses, but for cardiovascular responses to stressful events (Kayaba et al., 2003, Zhang et al., 2006a, Zhang et al., 2006b). Orexin neurons may behave differently depending on whether physiological activation is driven by spontaneous internal demands to stabilise normal daily life, or by unexpected external stimuli to cope with aversive events.

Orexin-related genetically modified animals for ultradian studies

So far, there are two major types of genetically modified animals for orexin study; orexin-knockout mice, and orexin-neuron-ablated transgenic mice/rats. Our previous studies have shown that the integrated daily-life ultradian patterns are preserved in transgenic rats (Mohammed et al., 2014). The main difference between the rats and this study on mice is that the ultradian episodic increases in body temperature were almost absent in ORX-KO mice but not in the transgenic rats. The discrepancy may be due to developmental compensation during orexin-neuronal degeneration that occurs during

juvenile periods (approximately 1-2 weeks after birth) in the transgenic rats. There may also be specie differences.

The issue with developmental compensation can be addressed by using new genetic mice models, in which the timing of initiation for the ablation process of orexin neurons can be controlled conditionally (Tabuchi et al., 2014), or by using another new model, in which orexin neuron can be temporally inhibited (Sasaki et al., 2011, Tsunematsu et al., 2013). Our preliminary data shows that conditional ablation of orexin neurons attenuates the amplitude of ultradian pattern in metabolism in a time dependent manner (Ootsuka et al., 2014).

Possible physiological role of the ultradian episodic pattern

In the wild, conservation of energy is a major concern for animals due to limited food resources. A fundamental approach to conserving energy is to sleep, as manifested in the Benington-Heller hypothesis, that sleep is a state for the restoration of brain energy metabolism (Benington and Craig Heller, 1995). During sleep, animals are highly vulnerable to attack from predators. Additionally, sleep results in a reduced opportunity for reproduction. Therefore, animals must wake occasionally in order to evaluate environmental risks and make assessments for survival. The phase-linked ultradian pattern may have evolved as a purposeful and dynamic physiological pattern to promote a desire for survival, although it is yet unknown why 1-2 hourly alternation has been selected. Orexin is unlikely to be necessary for promoting the desire, since ultradian eating patterns and the associated preparatory increases in arousal and heart rate were preserved in ORX-KO mice.

It has been suggested that an increase in body temperature during the active phase of ultradian patterning contributes to promoting arousal levels and facilitates complex brain functioning necessary for the daily life tasks such as foraging, which requires active engagement with the external environment (Janssen, 1992, Ootsuka et al., 2009, Blessing et al., 2012, Blessing and Ootsuka, 2016). If foraging occurs, it commences after the corresponding episodic increase in body temperature in mice and rats (Blessing et al., 2012). In the present study, ORX-KO mice were still able to forage without the preparatory increases in body temperature. The elevated body temperature during

sleep/resting in ORX-KO mice may explain the absence of the preparatory heating (Mochizuki et al., 2006).

Possible brain pathways mediating the ultradian episodic pattern

Polyphasic intra-daily activity patterns were described for many species. The concepts of ultradian patterning, however, have not drawn much attention from physiologists and even from chronobiologists, partly because the ultradian episodes are not regular cyclic events but non-stationary or stochastic patterns (Blessing et al., 2013, Blessing and Ootsuka, 2016). Thus, ultradian temporal organization has not been well investigated. We have demonstrated the highly-coordinated and phase-linked nature of increases in different behavioural and physiological parameters, strongly suggesting that the patterning is generated within the central nervous system (Ootsuka et al., 2009, Blessing et al., 2012, Blessing and Ootsuka, 2016). Some reports show ultradian neuronal activity in the suprachiasmatic nucleus that functions as a master clock for circadian rhythm (Hu et al., 2007, Hu et al., 2012). However, the destruction of the suprachiasmatic nucleus does not abolish ultradian patterns in behavioural and physiological parameters (Shiromani et al., 2004, Baker et al., 2005, Hu et al., 2007), suggesting that the suprachiasmatic nucleus is not part of ultradian pattern generation networks.

The orexin system, which is part of the arousal system, was relevant to this study as we were interested in analysing the activation/arousal phase of the ultradian pattern. If conserving energy by sleeping is a fundamental strategy for survival, the sleep system may have a predominant role in ultradian patterning. Importantly, suppression of the arousal system is not sufficient to increase the amount of sleep (Carter et al., 2010, Sasaki et al., 2011, Tsunematsu et al., 2011). Thus, focusing on the sleep system may be key to investigating brain mechanisms for ultradian patterning. A recent study has revealed that a sleep-active neuron group that contains melanin-concentrating hormone in the hypothalamus is important for sleep (Konadhode et al., 2013).

Conflict of interest statement

The authors declare that they have no conflicts of interest.

Acknowledgment

We thank Ms Miki Sakoda for technical assistance, Mr James Ang, Miss Isobel Doolette-Prunckun and Mr Andrew Parry for proof reading, Dr William Blessing for reviewing our manuscript, and Dr Aslak Grinsted for the MATLAB wavelet package. This research was supported by the Japan Society for the Promotion of Science, KAKENHI (23590280) and by National Health and Medical Research Council (1051826).

References

Alfoldi P, Rubicsek G, Cserni G, Obal F, Jr. (1990) Brain and core temperatures and peripheral vasomotion during sleep and wakefulness at various ambient temperatures in the rat. Pflugers Arch 417:336-341.

Antunes VR, Brailoiu GC, Kwok EH, Scruggs P, Dun NJ (2001) Orexins/hypocretins excite rat sympathetic preganglionic neurons in vivo and in vitro. Am J Physiol Regul Integr Comp Physiol 281:R1801-1807.

Aschoff J, Gerkema M (1985) On Diversity and Uniformity of Ultradian Rhythms. In: Ultradian Rhythms in Physiology and Behavior (Schulz, H. and Lavie, P., eds), pp 321-334: Springer-Verlag Berlin Heidelberg.

Baker FC, Angara C, Szymusiak R, McGinty D (2005) Persistence of sleep-temperature coupling after suprachiasmatic nuclei lesions in rats. Am J Physiol Regul Integr Comp Physiol 289:R827-838.

Bastianini S, Silvani A, Berteotti C, Elghozi JL, Franzini C, Lenzi P, Lo Martire V, Zoccoli G (2011) Sleep related changes in blood pressure in hypocretin-deficient narcoleptic mice. Sleep 34:213-218.

Bastianini S, Silvani A, Berteotti C, Lo Martire V, Cohen G, Ohtsu H, Lin JS, Zoccoli G (2015) Histamine Transmission Modulates the Phenotype of Murine Narcolepsy Caused by Orexin Neuron Deficiency. PLoS One 10:e0140520.

Benington JH, Craig Heller H (1995) Restoration of brain energy metabolism as the function of sleep. Prog Neurobiol 45:347-360.

Blessing W, Mohammed M, Ootsuka Y (2012) Heating and eating: brown adipose tissue thermogenesis precedes food ingestion as part of the ultradian basic rest-activity cycle in rats. Physiol Behav 105:966-974.

Blessing W, Mohammed M, Ootsuka Y (2013) Brown adipose tissue thermogenesis, the basic rest-activity cycle, meal initiation, and bodily homeostasis in rats. Physiol Behav 121:61-69.

Blessing W, Ootsuka Y (2016) Timing of activities of daily life is jaggy: How episodic ultradian changes in body and brain temperature are integrated into this process. Temperature 1-13.

Blum ID, Zhu L, Moquin L, Kokoeva MV, Gratton A, Giros B, Storch KF (2014) A highly tunable dopaminergic oscillator generates ultradian rhythms of behavioral arousal. Elife 3.

Bonnavion P, Jackson AC, Carter ME, de Lecea L (2015) Antagonistic interplay between hypocretin and leptin in the lateral hypothalamus regulates stress responses. Nat Commun 6:6266.

Buzsaki G, Moser EI (2013) Memory, navigation and theta rhythm in the hippocampal-entorhinal system. Nat Neurosci 16:130-138.

Carter ME, Yizhar O, Chikahisa S, Nguyen H, Adamantidis A, Nishino S, Deisseroth K, de Lecea L (2010) Tuning arousal with optogenetic modulation of locus coeruleus neurons. Nat Neurosci 13:1526-1533.

Chemelli RM, Willie JT, Sinton CM, Elmquist JK, Scammell T, Lee C, Richardson JA, Williams SC, Xiong Y, Kisanuki Y, Fitch TE, Nakazato M, Hammer RE, Saper CB, Yanagisawa M (1999) Narcolepsy in orexin knockout mice: molecular genetics of sleep regulation. Cell 98:437-451.

Chen CT, Hwang LL, Chang JK, Dun NJ (2000) Pressor effects of orexins injected intracisternally and to rostral ventrolateral medulla of anesthetized rats. Am J Physiol Regul Integr Comp Physiol 278:R692-697.

D'Olimpio F, Renzi P (1998) Ultradian rhythms in young and adult mice: further support for the basic rest-activity cycle. Physiol Behav 64:697-701.

Dowse H, Umemori J, Koide T (2010) Ultradian components in the locomotor activity rhythms of the genetically normal mouse, Mus musculus. J Exp Biol 213:1788-1795.

Gerkema MP, van der Leest F (1991) Ongoing ultradian activity rhythms in the common vole, Microtus arvalis, during deprivations of food, water and rest. J Comp Physiol A 168:591-597.

Graps A (1995) An Introduction to Wavelets. In: Computing in Science and Engineering.

Grinsted A, Moore JC, Jevrejeva S (2004) Application of the cross wavelet transform and wavelet coherence to geophysical time series. Nonlinear Proc Geoph 11:561-566.

Halasz P, Terzano M, Parrino L, Bodizs R (2004) The nature of arousal in sleep. J Sleep Res 13:1-23.

Hara J, Beuckmann CT, Nambu T, Willie JT, Chemelli RM, Sinton CM, Sugiyama F, Yagami K, Goto K, Yanagisawa M, Sakurai T (2001) Genetic ablation of orexin neurons in mice results in narcolepsy, hypophagia, and obesity. Neuron 30:345-354.

Holstein-Rathlou NH, He J, Wagner AJ, Marsh DJ (1995) Patterns of blood pressure variability in normotensive and hypertensive rats. Am J Physiol 269:R1230-1239.

Honma K, Hiroshige T (1978) Simultaneous determination of circadian rhythms of locomotor activity and body temperature in the rat. Jpn J Physiol 28:159-169.

Hu K, Meijer JH, Shea SA, vanderLeest HT, Pittman-Polletta B, Houben T, van Oosterhout F, Deboer T, Scheer FA (2012) Fractal patterns of neural activity exist within the suprachiasmatic nucleus and require extrinsic network interactions. PLoS One 7:e48927.

Hu K, Scheer FA, Ivanov P, Buijs RM, Shea SA (2007) The suprachiasmatic nucleus functions beyond circadian rhythm generation. Neuroscience 149:508-517.

Inutsuka A, Inui A, Tabuchi S, Tsunematsu T, Lazarus M, Yamanaka A (2014) Concurrent and robust regulation of feeding behaviors and metabolism by orexin neurons. Neuropharmacology 85:451-460.

Janssen R (1992) Thermal influences on nervous system function. Neurosci Biobehav Rev 16:399-413.

Kaur S, Thankachan S, Begum S, Blanco-Centurion C, Sakurai T, Yanagisawa M, Shiromani PJ (2008) Entrainment of temperature and activity rhythms to restricted feeding in orexin knock out mice. Brain Res 1205:47-54.

Kayaba Y, Nakamura A, Kasuya Y, Ohuchi T, Yanagisawa M, Komuro I, Fukuda Y, Kuwaki T (2003) Attenuated defense response and low basal blood pressure in orexin knockout mice. Am J Physiol Regul Integr Comp Physiol 285:R581-593.

Kleitman N (1982) Basic rest-activity cycle--22 years later. Sleep 5:311-317.

Konadhode RR, Pelluru D, Blanco-Centurion C, Zayachkivsky A, Liu M, Uhde T, Glen WB, Jr., van den Pol AN, Mulholland PJ, Shiromani PJ (2013) Optogenetic stimulation of MCH neurons increases sleep. J Neurosci 33:10257-10263.

Kuwaki T (2008) Orexinergic modulation of breathing across vigilance states. Respir Physiol Neurobiol 164:204-212.

Kuwaki T (2011) Orexin links emotional stress to autonomic functions. Autonomic Neuroscience 161:20-27.

Kuwaki T (2015) Thermoregulation under pressure: a role for orexin neurons. Temperature 2:379-391.

Leise TL (2013) Wavelet analysis of circadian and ultradian behavioral rhythms. Journal of circadian rhythms 11:5.

Leise TL, Indic P, Paul MJ, Schwartz WJ (2013) Wavelet meets actogram. J Biol Rhythms 28:62-68.

Livnat A, Zehr JE, Broten TP (1984) Ultradian oscillations in blood pressure and heart rate in free-running dogs. Am J Physiol 246:R817-824.

Lo Martire V, Silvani A, Bastianini S, Berteotti C, Zoccoli G (2012) Effects of ambient temperature on sleep and cardiovascular regulation in mice: the role of hypocretin/orexin neurons. PLoS One 7:e47032.

Machado BH, Bonagamba LG, Dun SL, Kwok EH, Dun NJ (2002) Pressor response to microinjection of orexin/hypocretin into rostral ventrolateral medulla of awake rats. Regul Pept 104:75-81.

Mahler SV, Moorman DE, Smith RJ, James MH, Aston-Jones G (2014) Motivational activation: a unifying hypothesis of orexin/hypocretin function. Nat Neurosci 17:1298-1303.

Mazzucchelli A, Conte S, D'Olimpio F, Ferlazzo F, Loizzo A, Palazzesi S, Renzi P (1995) Ultradian rhythms in the N1-P2 amplitude of the visual evoked potential in two inbred strains of mice: DBA/2J and C57BL/6. Behav Brain Res 67:81-84.

McGinty D, Szymusiak R (1990) Keeping cool: a hypothesis about the mechanisms and functions of slow-wave sleep. Trends Neurosci 13:480-487.

Mileykovskiy BY, Kiyashchenko LI, Siegel JM (2005) Behavioral correlates of activity in identified hypocretin/orexin neurons. Neuron 46:787-798.

Mochizuki T, Crocker A, McCormack S, Yanagisawa M, Sakurai T, Scammell TE (2004) Behavioral state instability in orexin knock-out mice. J Neurosci 24:6291-6300.

Mochizuki T, Klerman EB, Sakurai T, Scammell TE (2006) Elevated body temperature during sleep in orexin knockout mice. Am J Physiol Regul Integr Comp Physiol 291:R533-540.

Mohammed M, Ootsuka Y, Yanagisawa M, Blessing W (2014) Reduced brown adipose tissue thermogenesis during environmental interactions in transgenic rats with ataxin-3-mediated ablation of hypothalamic orexin neurons. Am J Physiol Regul Integr Comp Physiol 307:R978-989.

Monda M, Viggiano A, Mondola P, De Luca V (2001) Inhibition of prostaglandin synthesis reduces hyperthermic reactions induced by hypocretin-1/orexin A. Brain Res 909:68-74.

Monda M, Viggiano A, Viggiano A, Fuccio F, De Luca V (2004) Injection of orexin A into the diagonal band of Broca induces sympathetic and hyperthermic reactions. Brain Res 1018:265-271.

Nambu T, Sakurai T, Mizukami K, Hosoya Y, Yanagisawa M, Goto K (1999) Distribution of orexin neurons in the adult rat brain. Brain Res 827:243-260.

Nieminen P, Hohtola E, Mustonen A-M (2013) Body temperature rhythms in Microtus voles during feeding, food deprivation, and winter acclimatization. J Mammal 94:591-600.

Ono D, Honma K, Honma S (2015) Circadian and ultradian rhythms of clock gene expression in the suprachiasmatic nucleus of freely moving mice. Scientific reports 5:12310.

Ootsuka Y, de Menezes RC, Zaretsky DV, Alimoradian A, Hunt J, Stefanidis A, Oldfield BJ, Blessing WW (2009) Brown adipose tissue thermogenesis heats brain and body as part of the brain-coordinated ultradian basic rest-activity cycle. Neuroscience 164:849-861.

Ootsuka Y, Kulasekara K, de Menezes RC, Blessing WW (2011) SR59230A, a beta-3 adrenoceptor antagonist, inhibits ultradian brown adipose tissue thermogenesis and interrupts associated episodic brain and body heating. Am J Physiol Regul Integr Comp Physiol 301:R987-994.

Ootsuka Y, Miyata K, Ikoma Y, Kuwaki T, Yamanaka A (2014) The contribution of orexin to integrated ultradian physiological pattern. Australasian Neuroscience Society 34th Annual meeting SYM-09-02.

Poon AMS, Wu BM, Poon PWF, Cheung EPW, Chan FHY, Lam FK (1997) Effect of Cage Size on Ultradian Locomotor Rhythms of Laboratory Mice. Physiol Behav 62:1253-1258.

Price TS, Baggs JE, Curtis AM, Fitzgerald GA, Hogenesch JB (2008) WAVECLOCK: wavelet analysis of circadian oscillation. Bioinformatics 24:2794-2795.

Richter CP (1927) Animal Behavior and Internal Drives. The Quarterly Review of Biology 2:307-343.

Sakurai T (2007) The neural circuit of orexin (hypocretin): maintaining sleep and wakefulness. Nat Rev Neurosci 8:171-181.

Sakurai T (2014) The role of orexin in motivated behaviours. Nat Rev Neurosci 15:719-731.

Samson WK, Gosnell B, Chang JK, Resch ZT, Murphy TC (1999) Cardiovascular regulatory actions of the hypocretins in brain. Brain Res 831:248-253.

Sasaki K, Suzuki M, Mieda M, Tsujino N, Roth B, Sakurai T (2011) Pharmacogenetic modulation of orexin neurons alters sleep/wakefulness states in mice. PLoS One 6:e20360.

Shimada SG, Marsh DJ (1979) Oscillations in mean arterial blood pressure in conscious dogs. Circ Res 44:692-700.

Shiromani PJ, Xu M, Winston EM, Shiromani SN, Gerashchenko D, Weaver DR (2004) Sleep rhythmicity and homeostasis in mice with targeted disruption of mPeriod genes. Am J Physiol Regul Integr Comp Physiol 287:R47-57.

Silvani A, Bastianini S, Berteotti C, Cenacchi G, Leone O, Lo Martire V, Papa V, Zoccoli G (2014) Sleep and cardiovascular phenotype in middle-aged hypocretin-deficient narcoleptic mice. J Sleep Res 23:98-106.

Stupfel M, Damiani P, Perramon A, Busnel MC, Gourlet V, Thierry H (1985) Ultradian and circadian respiratory rhythms in grouped small laboratory vertebrate species as a method to assess the effects of environmental challenges. Comp Biochem Physiol A Comp Physiol 80:225-231.

Stupfel M, Gourlet V, Perramon A, Merat P, Court L (1990) Ultradian and circadian compartmentalization of respiratory and metabolic exchanges in small laboratory vertebrates. Chronobiologia 17:275-304.

Stupfel M, Gourlet V, Perramon A, Merat P, Putet G, Court L (1995) Comparison of ultradian and circadian oscillations of carbon dioxide production by various endotherms. Am J Physiol 268:R253-265.

Tabuchi S, Tsunematsu T, Black SW, Tominaga M, Maruyama M, Takagi K, Minokoshi Y, Sakurai T, Kilduff TS, Yamanaka A (2014) Conditional ablation of orexin/hypocretin neurons: a new mouse model for the study of narcolepsy and orexin system function. J Neurosci 34:6495-6509.

Terada J, Nakamura A, Zhang W, Yanagisawa M, Kuriyama T, Fukuda Y, Kuwaki T (2008) Ventilatory long-term facilitation in mice can be observed during both sleep and wake periods and depends on orexin. J Appl Physiol (1985) 104:499-507.

Torrence C, Compo GP (1998) A Practical Guide to Wavelet Analysis. Bulletin of the American Meteorological Society 79:61-78.

Tsujino N, Sakurai T (2009) Orexin/hypocretin: a neuropeptide at the interface of sleep, energy homeostasis, and reward system. Pharmacol Rev 61:162-176.

Tsunematsu T, Kilduff TS, Boyden ES, Takahashi S, Tominaga M, Yamanaka A (2011) Acute optogenetic silencing of orexin/hypocretin neurons induces slow-wave sleep in mice. J Neurosci 31:10529-10539.

Tsunematsu T, Tabuchi S, Tanaka KF, Boyden ES, Tominaga M, Yamanaka A (2013) Long-lasting silencing of orexin/hypocretin neurons using archaerhodopsin induces slow-wave sleep in mice. Behav Brain Res 255:64-74.

Willie JT, Chemelli RM, Sinton CM, Yanagisawa M (2001) To eat or to sleep? Orexin in the regulation of feeding and wakefulness. Annu Rev Neurosci 24:429-458.

Yamanaka A, Sakurai T, Katsumoto T, Yanagisawa M, Goto K (1999) Chronic intracerebroventricular administration of orexin-A to rats increases food intake in daytime, but has no effect on body weight. Brain Res 849:248-252.

Zhang S, Zeitzer JM, Sakurai T, Nishino S, Mignot E (2007) Sleep/wake fragmentation disrupts metabolism in a mouse model of narcolepsy. J Physiol 581:649-663.

Zhang W, Sakurai T, Fukuda Y, Kuwaki T (2006a) Orexin neuron-mediated skeletal muscle vasodilation and shift of baroreflex during defense response in mice. Am J Physiol Regul Integr Comp Physiol 290:R1654-1663.

Zhang W, Shimoyama M, Fukuda Y, Kuwaki T (2006b) Multiple components of the defense response depend on orexin: evidence from orexin knockout mice and orexin neuron-ablated mice. Auton Neurosci 126-127:139-145.

Zhang W, Sunanaga J, Takahashi Y, Mori T, Sakurai T, Kanmura Y, Kuwaki T (2010) Orexin neurons are indispensable for stress-induced thermogenesis in mice. The Journal of physiology 588:4117-4129.

Zhang W, Zhang N, Sakurai T, Kuwaki T (2009) Orexin neurons in the hypothalamus mediate cardiorespiratory responses induced by disinhibition of the amygdala and bed nucleus of the stria terminalis. Brain Res 1262:25-37.

Zheng H, Patterson LM, Berthoud HR (2005) Orexin-A projections to the caudal medulla and orexin-induced c-Fos expression, food intake, and autonomic function. J Comp Neurol 485:127-142.

Table 1

Physiological parameter	Dark phase	Light phase
Body temp inter-peak interval (min)	88±6	100±8 [ns]
Body temp amplitude (˚C)	1.1±0.1	1.0±0.1 [ns]
Time from onset to peak of body temp (min)	24±2	24±2 [ns]
Body temp at onset of increase (˚C)	35.5±0.4	34.6±0.4*
Heart rate amplitude (beats/min)	177±11	164±6 [ns]
Heart rate at onset of increase (beats/min)	437±9	431±12 [ns]
Activity amplitude (arbitrary)	637±58	541±77 [ns]

Table 2

		Dark phase	Light phase
WT	Number of meal per 12 hr	6±1	4±1
	Food eaten per meal (mg/10g weight)	83±9	61±8
	Total food eaten per 12 h (mg/10g weight)	496±86	223±54
KO	Number of meal per 12 hr	5±1 [ns]	2±1¶
	Food eaten per meal (mg/10g)	81±9 [ns]	94±17 [ns]
	Total food eaten per 12 hr (mg/10g)	388±106 [ns]	157±49 [ns]

Table legends

Table 1

Body temperature, heart rate and locomotor activity parameters (mean±SEM) associated with the ultradian episodic increase in wild type mice (n=8). Results from multiple ultradian episodes during the 24 hours recording period were averaged in individual mice, separately for 12-hour dark and 12-hour light phases, and the averaged data were pooled across mice. * significantly different from corresponding dark phase value by Student's paired t-test (; $t(7)=6.604$, $P<0.001$ for Body temp at onset of increase). ns not significantly different from corresponding dark phase value by Student's paired t-test ($t(7)=1.998$, $P=0.086$ for Body temp inter-peak interval; $t(7)=0.231$, $P=0.0824$ for Body temp amplitude; $t(7)=0.065$, $P=0.950$ for Time from onset to peak of body temp; $t(7)=1.114$, $P=0.302$ for Heart rate amplitude; $t(7)=0.734$, $P=0.487$ for Heart rate at onset of increase; $t(7)=1.516$, $P=0.173$ for Activity amplitude).

Table 2

Meal parameter for dark and light phases with ad libitum food in wild type mice (WT) (n=6), and in ORX-KO mice (KO) (n=5). The amount of food eaten was shown as gram per 10-gram body weight. ¶ significantly different from corresponding value of WT mice (For Number of meal per 12hr of Dark phase, $P=0.030$, Mann-Whitney U test). ns not significantly different from corresponding value of WT mice by Student's unpaired t-test (For Number of meal per 12 hr, $t(9)=1.204$, $P=0.259$ for Dark phase. For Food eaten per meal, $t(9)=0.153$, $P=0.882$ for Dark phase, $t(9)=1.765$, $P=0.111$ for Light Phase. For Total food eaten per 12, $t(9)=0.804$, $P=0.442$ for Dark phase, $t(9)=0.893$, $P=0.395$ for Light phase).

Figure legends

Figure 1

Body temperature (the top trace), hear rate (the middle trace), locomotor activity (the bottom trace) records in a wild type mouse under unanaesthetised and unrestricted condition. The contour maps above each trace were continuous wavelet-power spectrums. The colour changes as power increases of frequency components from blue to white. The significant wavelet-power areas were indicated by the pink contours. On original signal traces, yellow-filled and blue-filled circles indicate peak and onset times, respectively. These points were defined by the peak-method. The black and white bars at the bottom indicate light off (12 hours) and light on (12 hours), respectively.

Figure 2

Frequency distributions of time between peak of episodic increases in body temperature (A) and of amplitudes of the peaks (B) (129 episodes during 24 hours in 8 mice).

Figure 3

EEG Fourier-power (the top trace), body temperature (the second trace), heart rate (the third trace), food (the fourth trace), and locomotor activity (the fifth trace) records in a WT mouse under unanaesthetised and unrestrained condition. Continuous wavelet-power spectrum of EEG Fourier-power were shown above the EEG power trace. The colour changes as power increases of frequency components from blue to white. The significant wavelet-power areas were indicated by the pink contours. A broken line was place at the onset of each eating. The black and white bars at the bottom indicate light off (12 hours) and light on (12 hours), respectively.

Figure 4

Group data showing temporal inter-relationship between different physiological parameters plotted to the onset of each increase in body temperature (time zero, vertical dashed line) during the dark phase (A) and the light phase (B) from WT mice. Variables were first averaged in individual animals (dotted line) of 60 min records for each parameter, beginning 30 min before and after the peak time of ultradian episodes in body temperature and then pooled across all animals (thick line). Each thick trace was mean ±SEM (5min bins, n=6).

Figure 5

Group data showing temporal interrelation between different physiological parameters plotted to the onset time of eating, (time zero, vertical dashed line) during the dark phase from the WT mice (A) and from the ORX-KO mice (B). Variables were first averaged in individual animals (dotted line) of 60 min records of each parameter, beginning 30 min before and after the onset time of eating. Each thick trace was mean±SEM (5min bins, n=6).

Figure 6

Body temperature (the top trace), heart rate (the middle trace), locomotor activity (the bottom trace) records in one ORX-KO mouse under unanaesthetised and unrestricted condition. The contour maps above each trace were continuous wavelet-power spectrum. The colour changes as power increases of frequency components from blue to white. The significant wavelet-power areas were indicated by the pink contours. The black and white bars at the bottom indicate light off (12 hours) and light on (12 hours), respectively.

Figure 7

The continuous wavelet-power spectrum (A), and total wavelet-power of each parameter (B) from body temperature (top), heart rate (middle) and locomotor activity (bottom) in the WT (n=8) and the ORX-KO mice (n=8). **A**. Continuous wavelet-power spectrum of body temperature, heart rate and locomotor activity in the W mice (a) and the ORX-KO mice (b) from the telemetry-only-recording group. The colour-scaled z-axis shows the wavelet-power (magnitude of CWT) of the periodicity component. The black and white bars at the bottom of each graph indicate light off (12 hours) and light on (12 hours), respectively. **B**. Total wavelet-power of body temperature, heart rate, and locomotor activity in WT (white bar) and ORX-KO mice (shaded bar) from the CWT shown in A. Mean power was calculated in a periodicity band from 30 to 200 min at the first 6 hours of dark (D1) /light (L1) phase, and the second 6 hours of dark (D2) / light (L2) phase. The vertical bars represent standard deviation. * significantly smaller than corresponding values from the WT mice group (For body temperature, $t(14)=4.726$, $P<0.001$, Student's unpaired t-test for D1; $P=0.015$, Mann-Whitney U test for D2; $t(14)=2.997$, $P=0.01$, Student's unpaired t-test for L1; $t(9.206)=2.37$, $P=0.042$, Welch's test for L2. For heart rate, $t(14)=3.267$, $P=0.006$, Student's unpaired t-test for D1; $t(14)=1.052$, $P=0.311$ for D2; $t(14)=0.328$, $P=0.748$ for L1; $P=0.279$, Mann-Whitney U test for L2. For Activity, $t(14)=5.4$, $P<0.001$, Student's unpaired t-test for D1; $t(9.248)=4.224$, $P<0.002$, Welch's test for D2; $t(14)=0.142$, $P=0.142$, Student's unpaired t-test for L1; $t(14)=2.319$, $P=0.036$, Student's unpaired t-test for L2.).

Figure 8

EEG Fourier-power (the top trace), body temperature (the second trace), heart rate (the third trace), food (the fourth trace), and locomotor activity (the fifth trace) records in an individual ORX-KO mouse under unanaesthetised and unrestrained condition. Continuous wavelet-power spectrums of EEG were shown above the EEG power trace. The colour changes as power increases of frequency components from blue to white. The significant wavelet power areas were contoured by a pink line. A broken line was place at the onset of each eating. The black and white bars at the bottom indicate light off (12 hours) and light on (12 hours), respectively.

Figure 9

A. Continuous wavelet-power spectrum of EEG Fourier-power (1 min bin) in the WT mice (a) and the ORX-KO mice (b) from EEG recording group (n=6 for each genetic group). The colour-scaled z-axis shows the power (magnitude of CWT) of the periodicity component. The black and white bars at the bottom of each graph indicate light off (12 hours) and light on (12 hours), respectively.

B. Total wavelet-power of EEG Fourier-power in the WT and ORK-KO mice from continuous wavelet transformation shown in A. Mean power was calculated in a frequency band from 30 to 200 min at the first 6 hours of dark (D1) /light (L1) phase, and the second 6 hours of dark (D2) / light (L2) phase. The vertical bars represent standard deviation. * significantly smaller than corresponding values from the WT mice group (D1, $t(11)=2.671$, $P=0.022$, Student's unpaired t-test; D2, $P=0.022$, Mann-Whitney U test; L1, $P=0.022$, Mann-Whitney U test; L2, $t(11)=2.52$, $P=0.028$, Student's unpaired t-test).

Figure 1

Click here to download Figure: Fig1_MK29_WT_MATLABFit_final_IL.eps

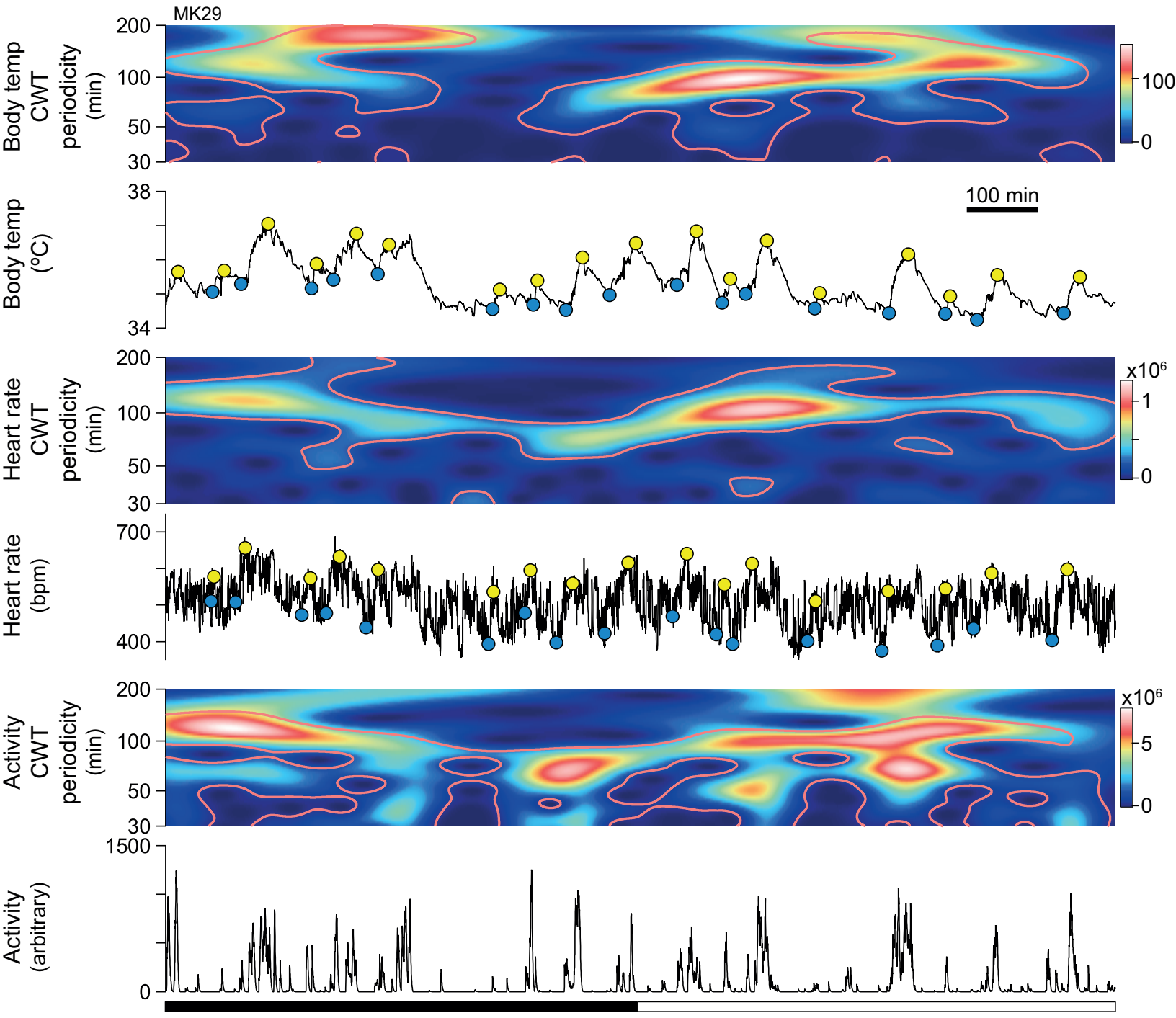

Fig. 1

Figure 2
Click here to download Figure: Fig2_final_IL.eps

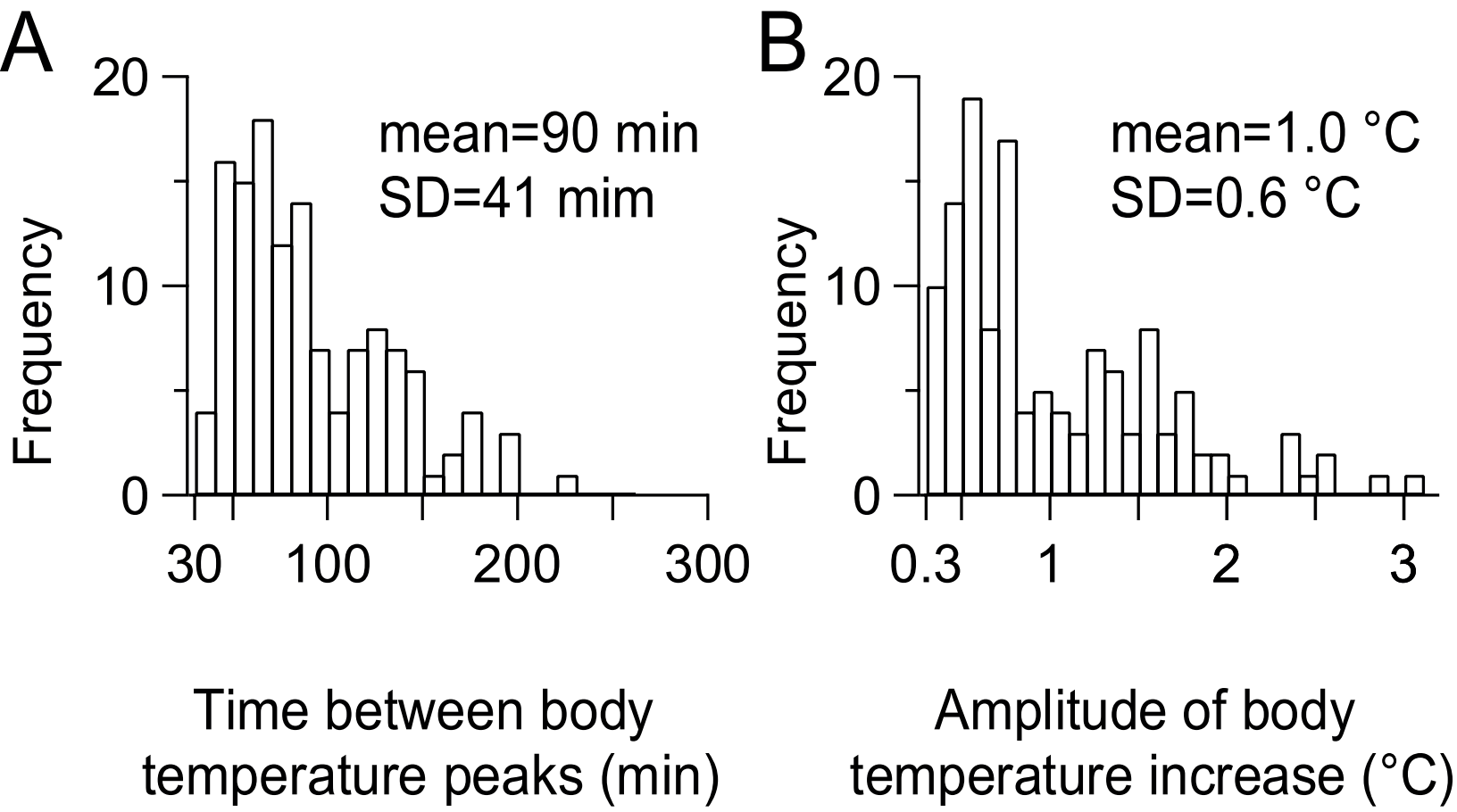

Fig 2

Figure 3

Click here to download Figure: Fig3_MK68_DL_layoutCWT_final_IL.eps

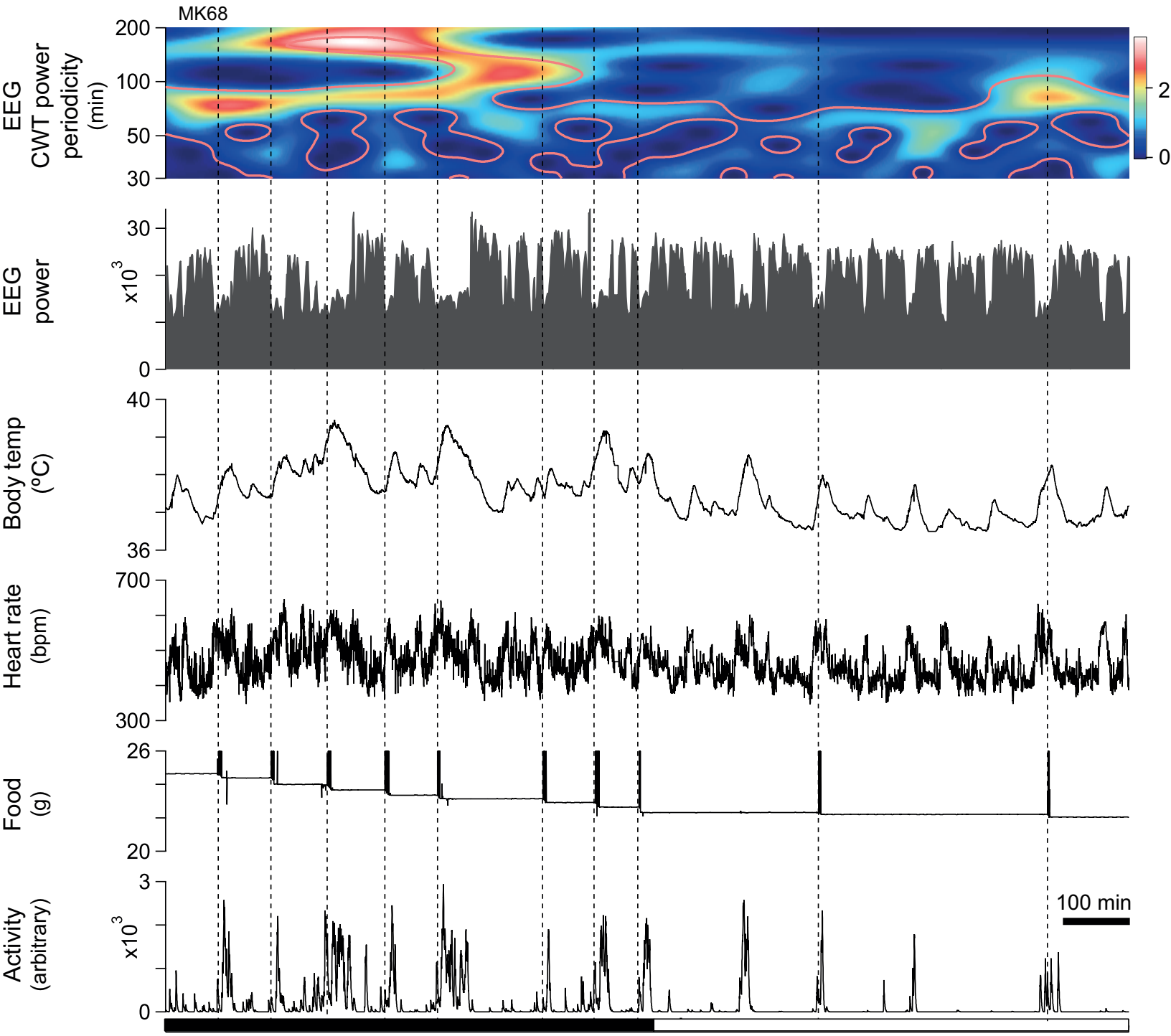

Fig. 3

Figure 4

Click here to download Figure: Fig4_WT_BodyON_timerelation_final_IL.eps

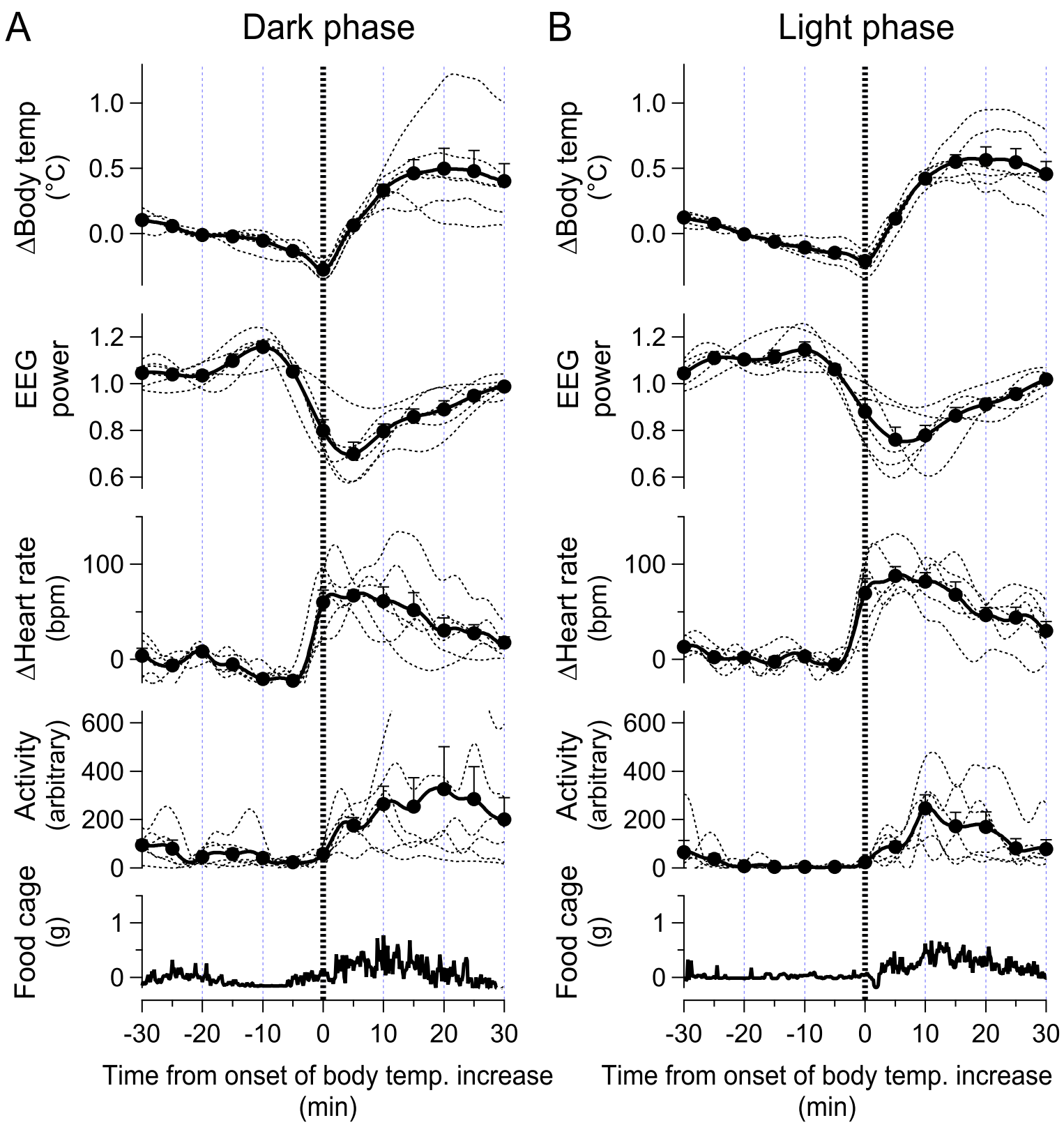

Fig. 4

Figure 5

Click here to download Figure: Fig5_WTKO_FoodON_timerelat_norm_final_IL.eps

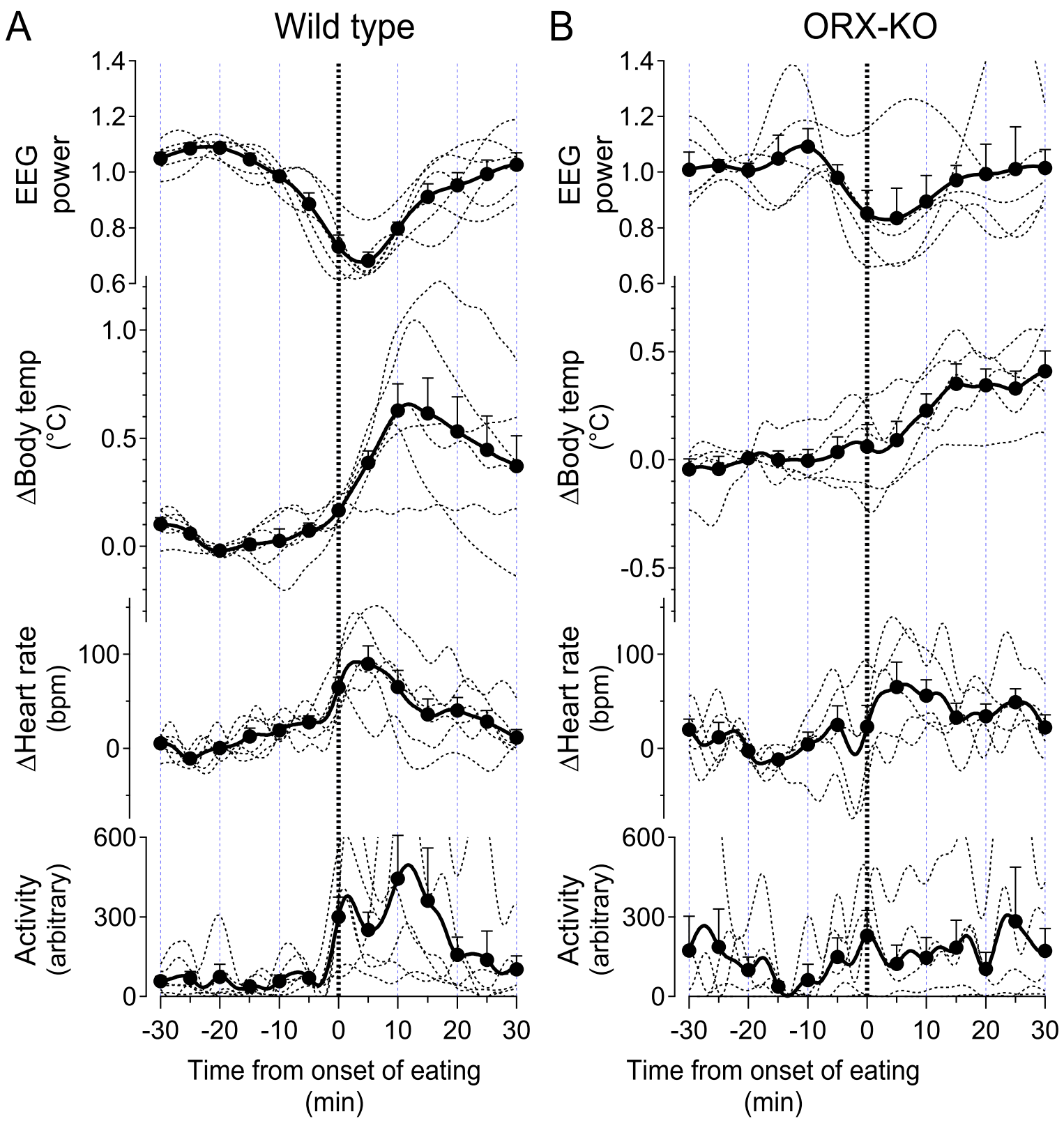

Fig. 5

Figure 6

Click here to download Figure: Fig6_KO_MK20_MATLABFit_final_IL.eps

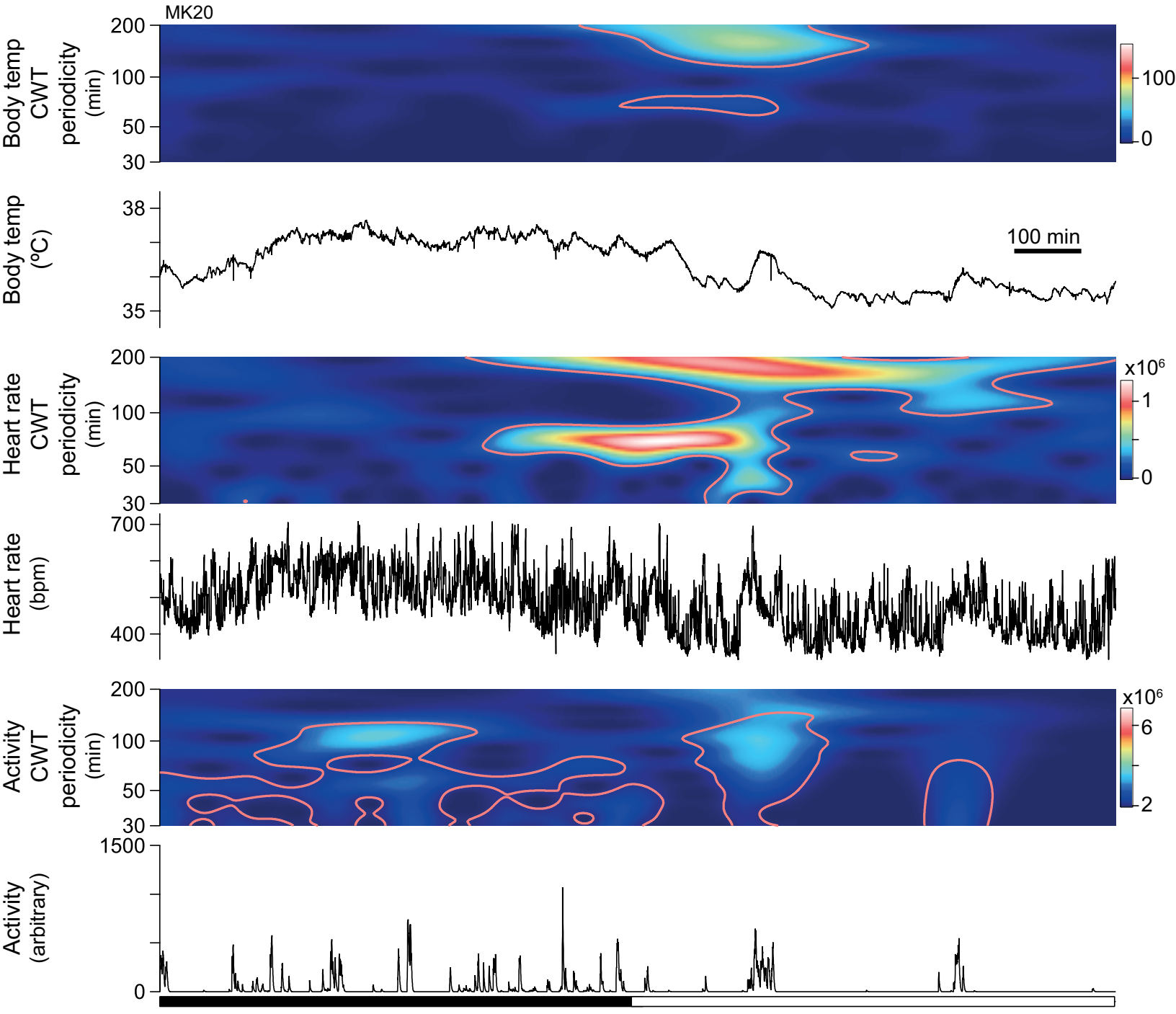

Fig. 6

Figure 7

Click here to download Figure: Fig7_Layout_without_sig_power_final_IL.eps

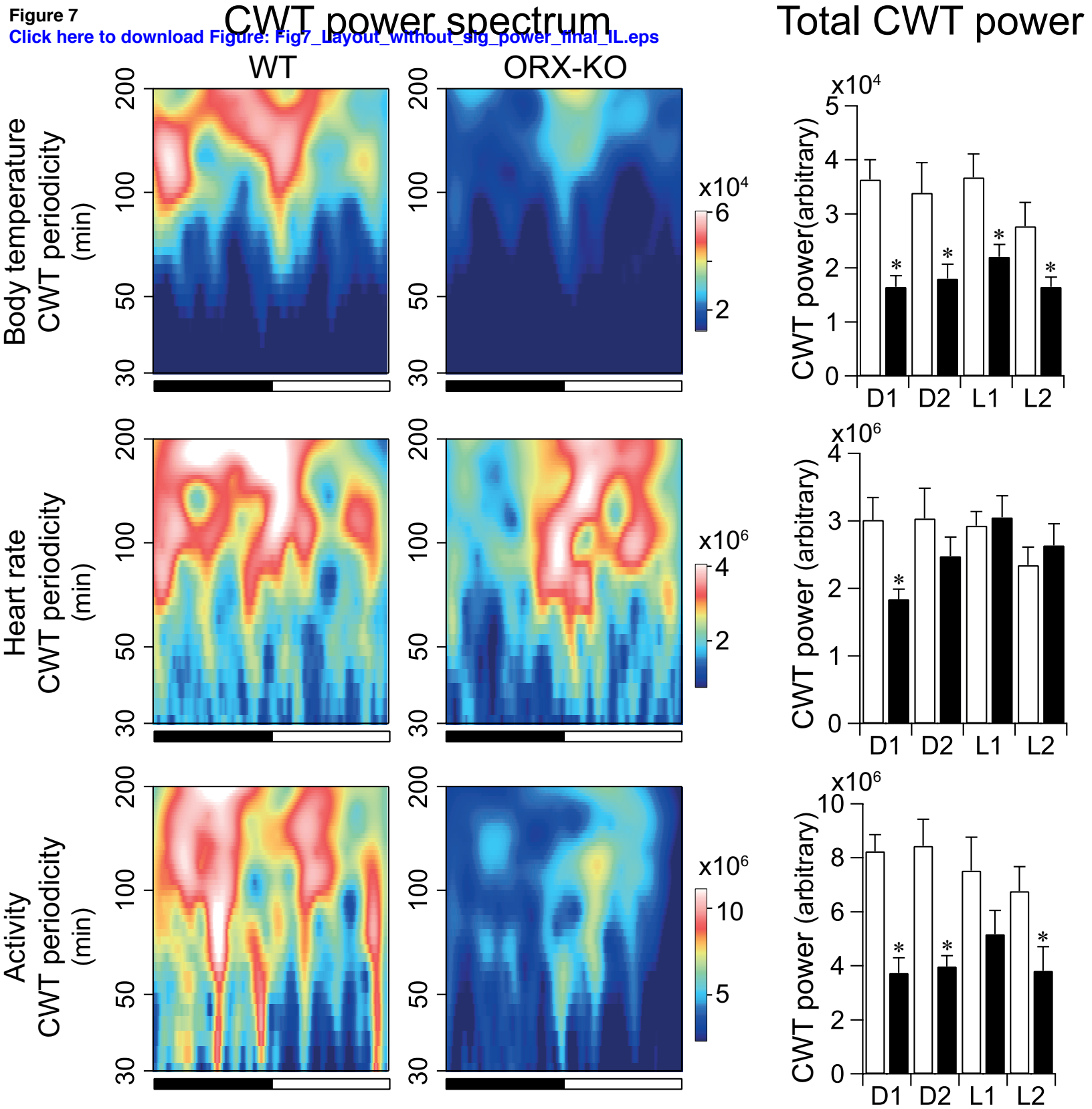

Fig 7

Figure 8

Click here to download Figure: Fig8_MK81_DL_layoutCWT_for_paper_final_IL.eps

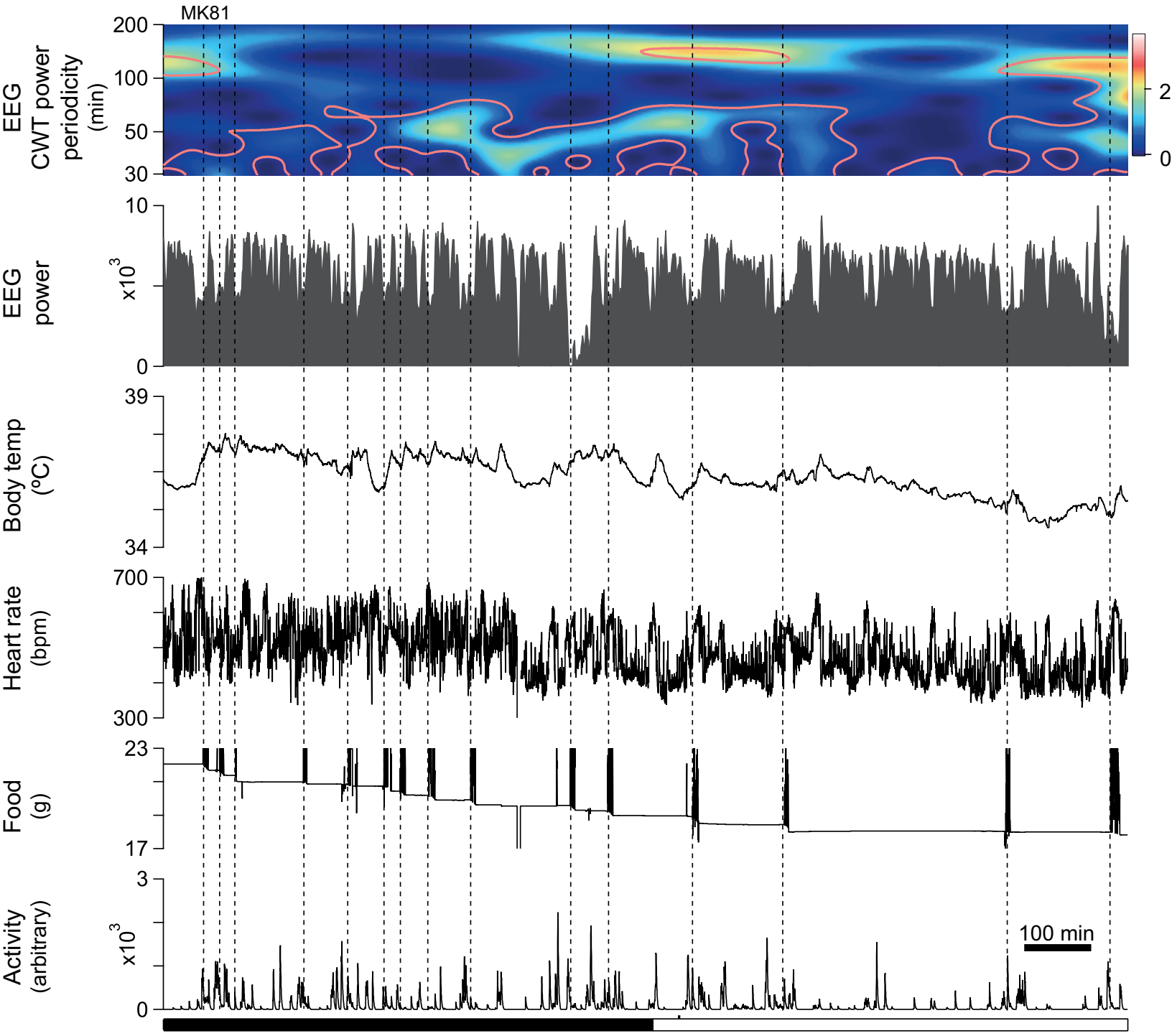

Fig. 8

Figure 9

Click here to download Figure: Fig9_EEGCWT_Zmean_log_noContour_final_IL.eps

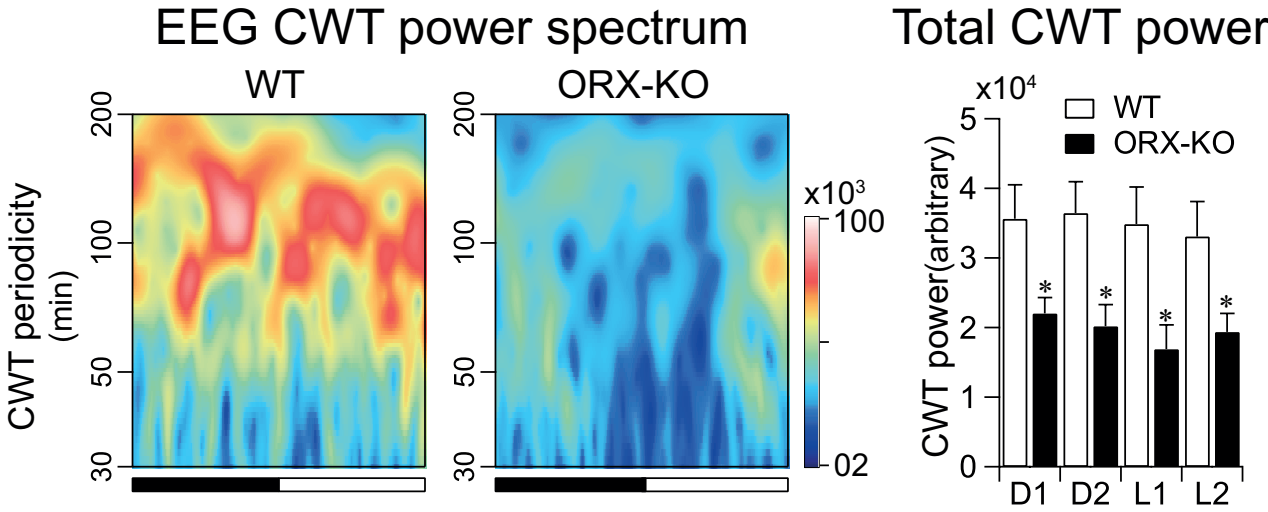

Fig 9